



Analyze of Frequency Selective Surfaces by Hybrid MOM-PO-GTD Method

Mendil Samir and Aguili Taoufik

École Nationale d'Ingénieurs de Tunis
e-mail: myemail.contact@gmail.com

Abstract - The intent of this article is to analyze the Diffraction phenomena of the incoming wave and provide a new Approach for analyzing the frequency selective surface (FSS) by using a hybrid method combining Moment Method (MoM), optical physics (PO) with General theory of Diffraction (GTD). The frequency selective surface (FSS) is a periodic surface with identical two-dimensional arrays of elements arranged on a substrate dielectric. An incoming plane wave will either be transmitted (bandwidth) or reflected (stopband), completely or partially, depending on the nature of the array element. This happens when the frequency of the electromagnetic (EM) wave correspond with the resonant frequency of the FSS elements. Hence, in free space, and for a certain frequency range, an FSS is capable of transmitting or blocking EM waves; therefore, identified as spatial filters. Today, FSSs have been extensively studied and there is tremendous growth in its design and implementation for different applications at the microwave to optical frequency ranges. In this review article, we present a new hybrid method form on Moment method and GTD for analyzing different categories of FSS based on the design of the structure, the array elements used, and applications. We also focus on the effects of diffraction, methodology, experimental verifications of design examples, as well as on prospects and challenges, particularly in the microwave regime. We highlight their important performance metrics, especially with regard to progress in this area could facilitate advanced electromagnetic innovation.

Keywords – Frequency selective surfaces; General theory of diffraction (GTD); microwave frequency; spatial filters; periodic structures.

Submission: July 2, 2019

Correction: January 27, 2020

Accepted: July 15, 2020

Doi: <http://dx.doi.org/10.14710/ijee.2.2.70-77>

[How to cite this article: Samir, M. and Taoufik, A. (2020). Analyze of Frequency Selective Surfaces by Hybrid MOM-PO-GTD Method. *International Journal of Engineering Education*, 2(2), 70-77. doi: <http://dx.doi.org/10.14710/ijee.2.2.70-77>]

1. Introduction

The Frequency Selective Surface FSSs mark their presence in many applications, including reflectors, antenna radomes, radar-absorbing materials, polarizers and composite metamaterials. Since this area of research is relatively old, but extremely fast-growing, it carries a wide range of applications and theories as many design and analysis tools have been developed. However, significant problems related to the theoretical and practical importance still have to be solved, and requires more work for example the development of double-curve FSS, non-periodic FSS.

According to the definition given in [1], FSS are metasurfaces that simply present an electrical response [2]. Since to adapt the frequency selectivity to the transmission/reflection characteristics, only the electric polarization can be sufficient. Conforming to the theory of antenna and microwave engineering, these surfaces are made by planar and periodic networks of metal patches of different shapes. The patch has a negligible thickness compared to the wavelength, although it is large enough contrast with the depth of the skin of the metal. Both, meta-materials and metasurfaces (MSs) are fast-growing areas of re- search,

with their use, spatially varying EM or optical responses can be obtained at will, with diffusion phase, amplitude, and polarization. Through a good selection of materials and design, the ultra-thin structure of MSs can suppress the detrimental and undesirable losses in the direction of wave propagation. When the considering polarization response, all metasurfaces can be classified on the basis of the operating principle of a matrix element, i-e their functionalities (frequency selective surfaces (FSS), high impedance surfaces, perfect absorbers, reflective surfaces, etc.). Therefore, such a structure can perfectly be estimated as a tiny network of perfect conductive resonant elements. This approximation is applied to the complementary structures of the FSSs i-e aperture, with it faces a limitation when the surface of the aperture cell becomes equal to the elementary cell (mesh type). Square and hexagonal mesh cells have generally been used and are also referred to as a capacitive grid. The existence of the resonance size of the array element causes the emergence of side lobes in the transmitted and reflected fields, which are the defining characteristic of FSS. However, compared to the FSS, the resonant element and the elementary cell of the metasurface

are relatively much smaller than the wavelength and allow the elimination of grating lobes in the frequency response. Therefore, FSS in the terahertz domain is usually called metasurfaces [3]. In recent years, dispersion properties of FSS have been explored using approximate analytical techniques, which imply an equivalent circuit method (GEC) for analyzing the characteristics of the transmission line (quasi-static approximation). However, with the growth of more complex structures, advanced numerical methods have been introduced that use periodic boundary conditions (PBCs) allowing for a fairly simple design analysis. Some of them include the finite element method (FEM), the moment method (MoM), the finite-difference time domain method (FDTD) and the integral equation method (boundary element) (IEM / BEM) [4-10]. A well-known technique is the IEM / BEM used in combination with MoM [11-14]. Various designs of FSSs and schemes for examining their SE characteristics are well presented in [2].

Therefore, in free space, and for certain frequency range, an FSS is capable of transmitting or blocking EM waves; styling Diffraction phenomena of these EM waves and its interaction with the complex form of this structures explored more the properties of FSS and correct some parameters.

This paper targets to

- The link among their crucial theoretical, structure geometry and significant performance parameters due to Diffraction phenomena analyze;
- A joining numerical method with asymptotic one General Theory Of Diffraction (GTD) in the new approach of analyzing;
- Highlight the important of Diffraction phenomena on their performance.

2. Study of Diffraction of Incident Wave in FSS Structure based on "metallic frame"

In this section, we choose to study at the beginin a simple form "metallic frame" as FSS element presented in fig.1.

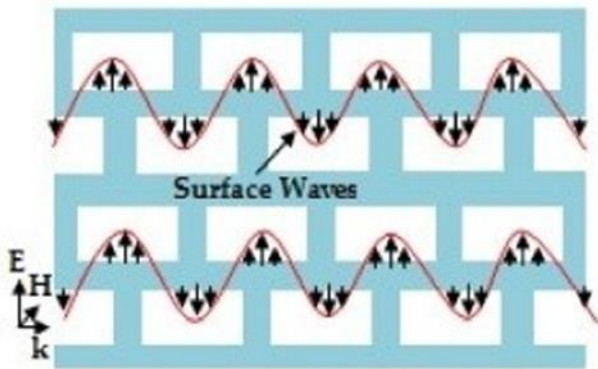


Figure 1: Surface waveguide made of metallic frames

Periodic perfectly conducting surfaces of electricity (PEC) are the easiest to understand theoretically, because

they admit only sources of electrical current J. This section presents the method of the spectral domain for the analysis of a PEC FSS in a free-standing (without substrate). The electric field E is linked to the magnetic vector potential A via the equation:

$$E = -jk\eta[A + \frac{1}{k^2}\nabla(\nabla \cdot A)](1)$$

and the vector magnetic potential is:

$$\nabla^2 A + k^2 A = -J(2)$$

With:

$$k^2 = \omega^2(\mu\epsilon) = (\frac{2\pi}{\lambda})^2$$

Frequency selective surfaces are frequently stratified in the normal direction to the plane of the surface. In other words, all dielectrics are stratified and all metal conductors are also considered stratified, and they will be considered perfectly planar. As a result, we exclude metal (wires perpendicular to the FSS plane) that could potentially connect currents from different layers of the FSS structure. With this kind of stratified structure in mind, we can then use a plane wave extension for the fields inside and around the FSS, because plane waves are the eigenfunction of the equations of vector waves in a media without source.

We consider an infinite 2D periodic surface occupying the entire x-y plane, and assume a discrete plane wave expansion for all currents, fields and potentials to solve equations (4) and (3) for a free-standing, doubly periodic surface:

$$J(x, y, z) = \sum_{mn}^N J(\alpha_m, \beta_n) \exp^{j(\alpha_m x + \beta_n y + \gamma_{mn} z)}(3)$$

$$E(x, y, z) = \sum_{mn}^N E(\alpha_m, \beta_n) \exp^{j(\alpha_m x + \beta_n y + \gamma_{mn} z)}(4)$$

$$A(x, y, z) = \sum_{mn}^N A(\alpha_m, \beta_n) \exp^{j(\alpha_m x + \beta_n y + \gamma_{mn} z)}(5)$$

To simplicity, we assume a rectangular lattice in which α only depends on m and β only depends on n. In the equations above, we have:

$$\alpha_m = k \sin(\theta_0) \cos(\phi_0) + \frac{2m\pi}{l_x}(6)$$

$$\beta_n = k \sin(\theta_0) \sin(\phi_0) + \frac{2n\pi}{l_y}(7)$$

$$\gamma_{mn} = \sqrt{k^2 - \alpha_m^2 - \beta_n^2}(8)$$

With, l_x and l_y dimation of the unit cell in (x-y), $k = 2\pi/\lambda$: wavelength, θ_0, ϕ_0 are the direction of an incident plane wave with the FSS regarded as lying in the x-y plan. The γ_{mn} called the root, taken which has a positive real part and non-positive (i.e., either negative or zero) imaginary

part). Now, for obtaining the Integral equation for free-standing PEC FSS, substituting equations (3-5) into (1) and (2) yields the spectral domain Greens function relating the radiated electric field to its source currents, where we consider only those components of the field vectors lying in the plane of the FSS, the x-y plane.

$$E(\alpha_m, \beta_n) = \frac{j k \eta}{\sqrt{k^2 - \alpha_m^2}} G_{mn} J(\alpha_m, \beta_n) \quad (9)$$

where

$$G_{mn} = \begin{bmatrix} 1 - \frac{\alpha_m^2}{k^2} & -\frac{\alpha_m \beta_n}{k^2} \\ -\frac{\alpha_m \beta_n}{k^2} & 1 - \frac{\beta_n^2}{k^2} \end{bmatrix} \quad (10)$$

Here we notice the singularity of the branch point in the equation above (the inverse singularity of the square root), which is not a problem thanks to the discrete spectrum, as long as the wavelength is not never equal to the spacing of the cells in our case $\lambda < (D_x, D_y)$. With this, the boundary condition of the electric field at the surface of the PEC material in a unit cell becomes

$$-E^{inc}(x, y) = \sum_{mn} \frac{1}{\sqrt{k^2 - \alpha_m^2 - \beta_n^2}} G_{mn} J(\alpha_m, \beta_n) \exp^{j(\alpha_m x + \beta_n y)} \quad (11)$$

$$E^{inc}(x, y) = E^{inc}(\alpha_0, \beta_0) \exp^{j(\alpha_0 x + \beta_0 y)} \quad (12)$$

Again, we limit our attention to the x, y components of currents and fields, which lie in the plane of the diffuser. Equation (14) is not strictly correct because only the tangential components of the electric field are really zero on the surface of the PEC diffusers. This inaccuracy will be solved now when (14) will be tested with the current basic functions, defined as residing on the surface of the diffuser.

In the followin we begin to study a diffraction phenomina for a single element of FSS, as presented in figure 2.

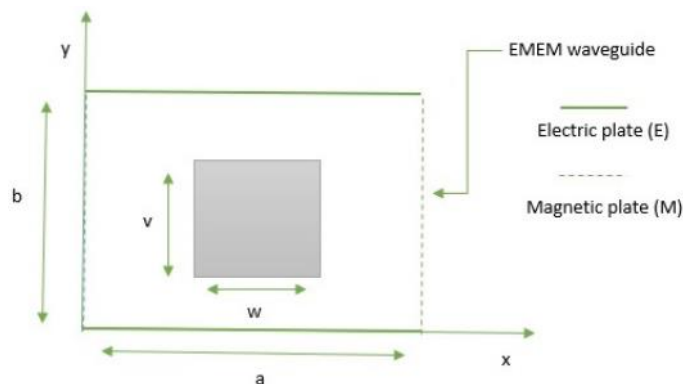


Figure 2. Single Cell of FSS in waveguide

2.1 New Approach MOM-PO-GTD

2.1.1 Calcul of Optical Physics (J_{PO}) Current

We propose to determine the first step of the new test function by the optical physics method. This approach is based on the determination of the current flowing through the metal when it is illuminated by an electromagnetic field as we see in figure 3.

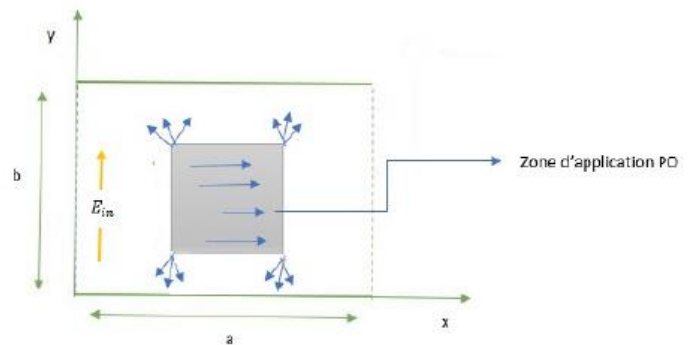


Figure 3. Mechanism of Optical Physics on the FSS unit

E_{inc} and H_{inc} electric and magnetic fields associated with the fundamental mode of the waveguide (TEM). Like the surface of an object illuminated by an incident magnetic field H_{in} , an electric current density called J_{PO} found in this surface this current in related to the magnetic field by the following equation.

$$\vec{J} = 2 \vec{H}_{in} \wedge \vec{z} \quad (13)$$

with H_{in} the incident magnetic field on the waveguide. \vec{y} the unit normal vector. The H_{in} related to the incident electric field by:

$$\text{rot}(\vec{E}_{inc}) = -i\omega\mu_0 \vec{H}_{in} \quad (14)$$

the current is evaluate as:

$$\vec{J}_{po} = \frac{2\beta}{\omega\mu_0} \sqrt{\frac{1}{a}} \vec{y} \quad (15)$$

β is the waveguide constant of propagation, ω the wave pulsation and μ_0 the permeability of the air.

2.1.2 Calcul of General diffraction theory Current (J_{GTD})

Diffraction it's considered as a local phenomenon at very high frequencies, the GTD relies on known solutions of diffraction such as diffraction by half-plane, dihedral, cone, cylinder. From these solutions in the far field, we propose to build an asymptotic evaluation of J_{GTD} that converge better to the exact solution.

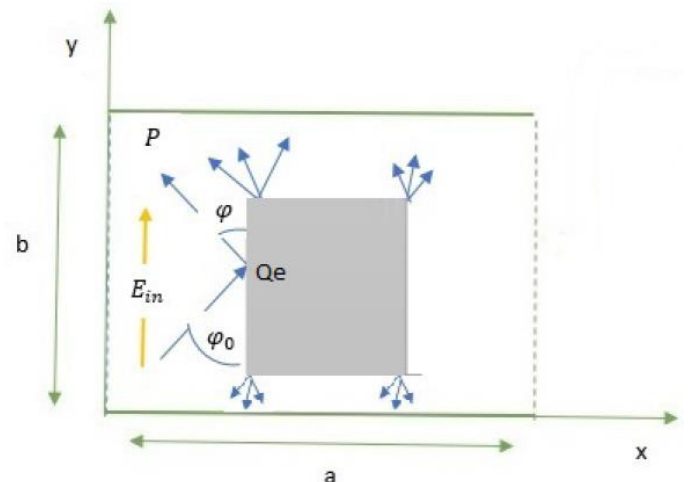


Figure 4. Diffraction of incident wave on the Edge and tips of the FSS unit

In the figure 4, a plane wave at normal incidence at the point P can be expressed in TEM fundamental Mode as:

$$E^i = \frac{1}{\sqrt{a}} \exp^{-jkz} \quad (16)$$

the incident electric field E^i may be decomposed into component parallel to the plane of incidence $E_{||}^i = \hat{\phi}_0 E^i$, and a component perpendicular to the plane of incidence $E_{\perp}^i = \hat{\phi} \cdot E^i$. Thus,

$$E^i = \hat{\phi}_0 E_{||}^i \quad (17)$$

and

$$H^i = \hat{\phi}_0 H_{\perp}^i \quad (18)$$

$$E_{||y}^i = \hat{y} \cdot E_{||}^i = (\hat{\phi}_0) \sin(\phi_0) \quad (19)$$

For magnetic field,

$$H_{\perp x}^i = \sqrt{\frac{\mu}{\epsilon}} (\hat{\phi} \cdot E^i) \sin(\phi_0) \quad (20)$$

The electromagnetic plane wave incident on the perfectly-conducting wedge, the total electric field intensity E and the total magnetic field intensity H in the region surrounding the wedge composed into a total of transverse and axial (to x^*). Referred to P.H Pathak and R.G kouyoumjian work, the field diffracted by this edge will be:

$$E_y^d = E_y^i \sqrt{\sin \phi_0} D \frac{\exp^{-jk_t \rho}}{\sqrt{\rho}} \exp^{-jk_t z} \quad (21)$$

and

$$H_x^d = H_x^i \sqrt{\sin(\phi_0)} D \frac{\exp^{-jk_t \rho}}{\sqrt{\rho}} \exp^{-jk_t z} \quad (22)$$

where E_y^i and H_x^i are evaluated at Q_E , the point of incidence on the edge, we must calculate the following Coefficient:

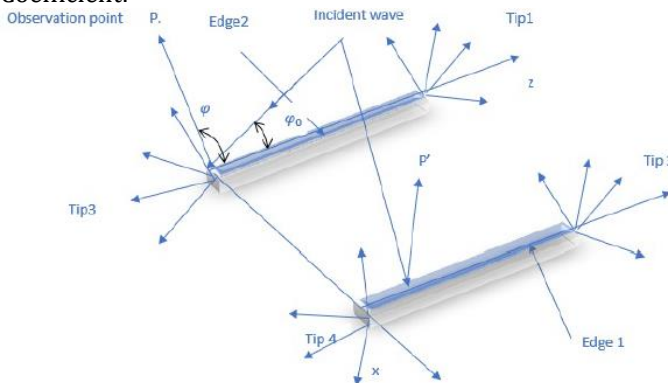


Figure 5. Modelization of FSS unit Edge and tips

From figure 5, the fine metal wire with b radius and l length we introduce their diffractions coefficients.

For thin edge:

$$D_{edge} = \frac{\exp^{i\frac{\pi}{4}}}{\sqrt{\frac{\pi}{2ksin^2\phi_0} \frac{1}{\gamma + \log(\frac{kbsin\phi_0}{2j})}}} \quad (23)$$

with $\gamma = 0.577$ is the Euler constant. and ϕ_0 is angle between tangent to the edge and incident wave, b and l is respectively the radius and the length of this fine edge, we assume in the follows that the product of wire radius b and the wave number k is small and we are justified in neglecting the terms $O((kb)^2) \ln(kb)$.

For the tips:

$$D_{tip} = \frac{1}{k} \frac{2ln \frac{2i}{\gamma kbsin\phi_0} ln \frac{2i}{\gamma kbsin\phi}}{ln \frac{2i}{\gamma kbsin(\frac{\phi_0}{2})} ln \frac{2i}{\gamma kbsin(\frac{\phi}{2})}} - \frac{tg(\frac{\phi_0}{2})tg(\frac{\phi}{2})}{\cos(\phi) + \cos(\phi_0)} \quad (24)$$

with $n=3$.

finally the diffraction coefficient is defined as :

$$\bar{D} = 2D_{edge} + 4D_{tips} \quad (25)$$

The total diffracted field around the structure is expressed as :

$$E_d^t = E_{edge1}^d + E_{edge2}^d + E_{tip1}^d + E_{tip2}^d + E_{tip3}^d + E_{tip4}^d \quad (26)$$

Or

$$rot(E_d^t) = -i\omega\mu_0 \vec{H}_d \quad (27)$$

Then,

$$J_{gtd} = (\vec{H}_d + \vec{H}_i) \wedge \vec{z} \quad (28)$$

The GTD current is concluded by the following expression:

$$\vec{J}_{gtd} = \frac{\beta}{\omega\mu_0} \left[\frac{1}{\sqrt{a}} (2D_{edge} + 4D_{tip}) + 2\sqrt{\frac{1}{a}} \right] \vec{y} \quad (29)$$

then, the total current J_t is composed by J_{po} as first part, and J_{GTD} second part, $J_t = J_{po} + J_{GTD}$ and it will be used as a single test function in our hybrid method.

$$\vec{J}_t = \left[\left(\frac{\beta}{\omega\mu_0} \left[\frac{1}{\sqrt{a}} (2D_{edge} + 4D_{tip}) + 2\sqrt{\frac{1}{a}} \right] \right) + \frac{2\beta}{\omega\mu_0} \sqrt{\frac{1}{a}} \right] \vec{y} \quad (30)$$

As we see we notice the appearance of the coefficients of diffractions in the expression of the current J_t , therefore, we highlight, the effect of the geometry (edge, tips, etc.) of the structure of study. According to the Galerkin's method, to determinate a structure's input impedance and distributions of field and current, a number of projections between test and basis functions (g_p, f_m) must be achieved.

Considering our approach, the single test function is divided into two parts ($J_t = J_{po} + J_{gtd}$), its projection on the waveguide's basis functions lead to obtaining the two integrals in the following:

$$\langle J_t, f_m \rangle = \langle J_{po}, f_m \rangle + \langle J_{gtd}, f_m \rangle \quad (31)$$

$$\langle J_t, f_m \rangle = \int_{x_1}^{x_2} \int_{y_1}^{y_2} f_m J_{po} dx dy + \int_{x_1}^{x_2} \int_{y_1}^{y_2} f_m J_{gtd} dx dy \quad (32)$$

For J_{gtd} Current, the width of the edge is very small, assimilated to wire antenna, then we have a variation according to y .

$$\langle J_{gtd}, f_m \rangle = \int_{y_1}^{y_2} f_m J_{gtd} dy \quad (33)$$

To simplify the calculation of the equation (31), we will solve it numerically using the rectangle method (midpoint method) expressed as:

$$\int_{y_1}^{y_2} f(y) dy = \sum_{i=1}^n f(y_i) dy \quad (34)$$

We've studied up to now only one element of the FSS structure, to have the whole just substituting (32), according the simplification and the boundary condition, into (11), and we consider that all unit spacing by l_x et l_y great than wavelength to eliminate the effect coupling in FSS structure, we obtain

$$\sum_j \left[\sum_{mn} \frac{J_t(-\alpha_m, -\beta_n) G_{mn} g_j(\alpha_m, \beta_n)}{\sqrt{k^2 - \alpha_m^2 - \beta_n^2}} \right] = -J_t(-\alpha_0, -\beta_0) \cdot E^{inc}(\alpha_0, \beta_0) \quad (35)$$

3. Numerical Results and Discussion

3.1 Convergence study

In our problem, we use a single test function, so the convergence study is done as a function of Number of modal basis functions. We present in the fig.6 the input impedance Z_{in} of the considered structures against number of modes of waveguides in the frequency range [10Ghz,12Ghz]. It is clear that for all structures, the Z_{in} 's convergence is obtained for 100 modes of waveguides. We note that the convergence is rapidly reached compared to cases using sinusoidal or trimgular test functions. This conforms with the law ($\frac{P}{N} < \frac{M_{\text{total sur face}}}{\text{total sur face}}$) in a domain of discontinuity, with P is test functions Number and N is basis functions Number.

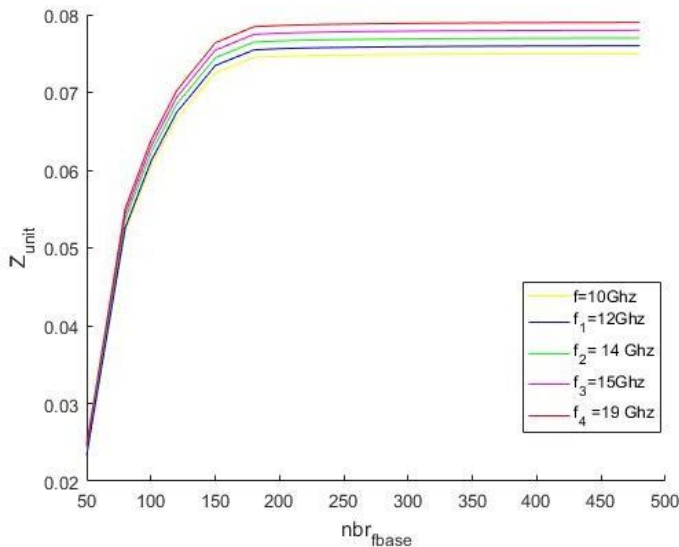


Figure 6. Input Impedance for different Number of Basics Function

3.2 Gain and Comparison between (MoM) Method and Hybrid method

In order to evaluate our approach, we will compare for FSS structures, the results provided by the method of the moments using the functions of the sinusoidal tests, for the

input impedance and the distribution of the current with those find by the hybrid method.

At beginning, the real and imaginary part of input impedances is computed for the frequency range [10Ghz, 12Ghz] and drawn in figure 7 and figure 8.

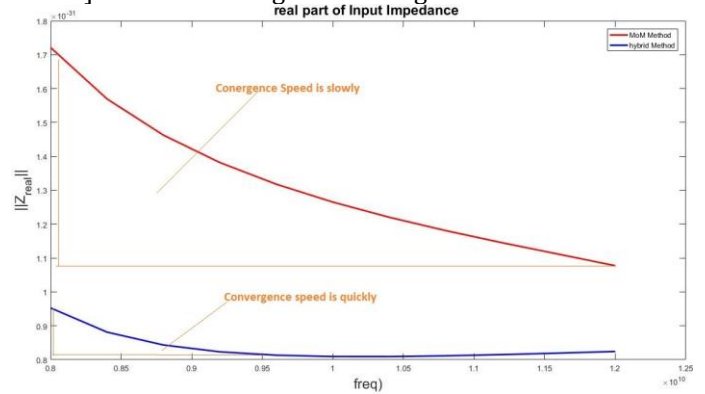


Figure 7. Comparison between MoM Method and Hybrid Method of Real Part of Input Impedance on the FSS Element

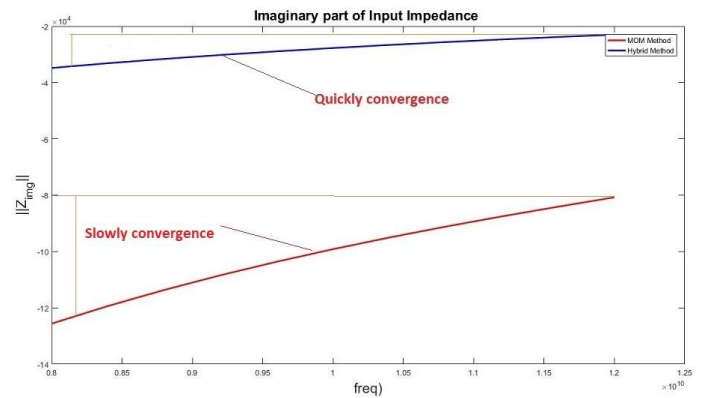


Figure 8. Comparison between MoM Method and Hybrid Method of Imaginary Part of Input Impedance on the FSS Element

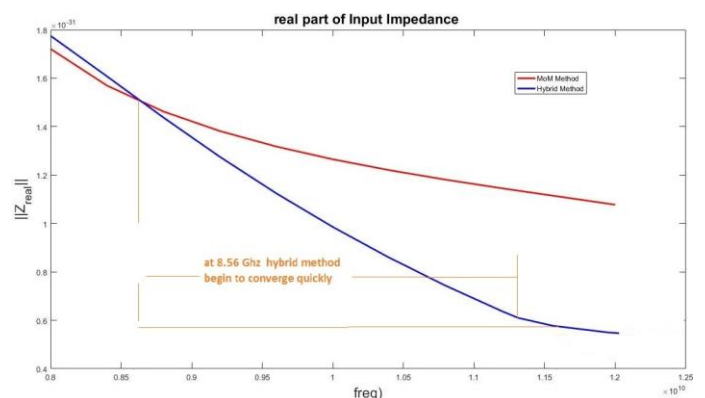


Figure 9. Real Part of Input Impedance with all Diffraction Coefficient on the FSS Element

to highlight the importance of the geometries shape with draw in fig 7 the real part of input impedance for hybrid method with only the diffraction made by the edge, and in fig 9 we draw the real part of input impedance with all

diffraction coefficient, and we demonstrate here, that the hybrid method converge quickly than others. For the structure, the obtained results by the two methods are in agreement for the frequency in the previous range. We reporting here, that the numbers of sinusoidal test and basis functions used for MoM method are respectively 40 and 3000 for the structure, whereas our approach consists in using only one hybrid test function with 100 basis functions. Another very important remark is that the speed of the convergence of our hybrid approach is very fast compare by the moments method its clear in the slopes of the two curves fig7a or fig 8, caused essentially by the diffraction coefficients used. The convergence is achieved quickly since the number of test and basis functions is decreases the number of operation are reduced also.

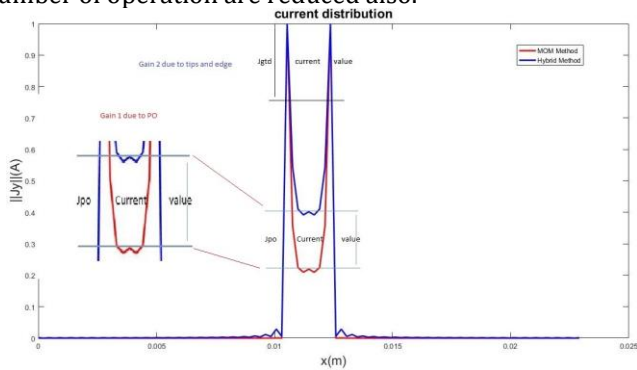


Figure 10. Comparison between MoM Method and Hybrid Method of Current Distribution on the FSS Element

The Hybrid current distribution given in the fig 10 and its compared to those obtained with MoM method. A good agreement between the two methods is assured. It is also clear that the current on edges, approximated by the asymptotic method GTD using the diffraction coefficient, will satisfy boundary conditions: its maximum on the edge of each FSS element. This demonstrates the development of the proposed test function.

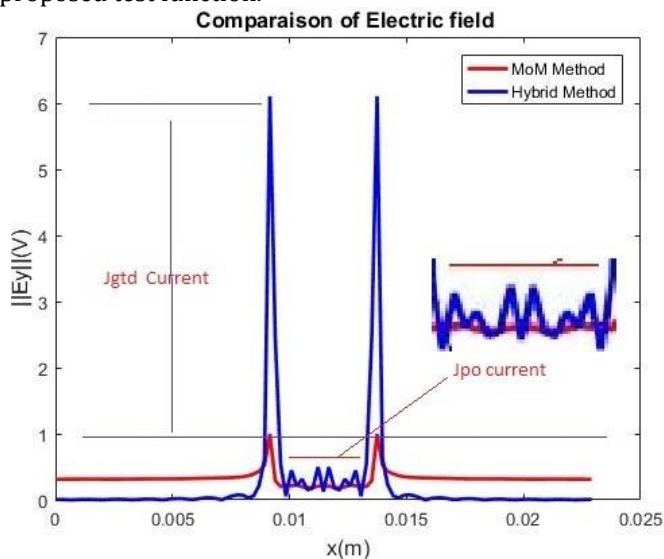


Figure 11. Comparison between MoM Method and Hybrid Method of Electric Field on the FSS Element

Similarly, fig.11 shows the electric fields distribution. Like input impedances and current, there is a perfect accordance between the two methods with verification of boundary conditions. In further, the intensity of the electric field is very high in hybrid method, caused essentially by the secondary source (tips, edge) that its accounting in our approach, and negligent in Moment method. The number of basis functions is reduced too (no more calculate operation to do), and a good accuracy of the new hybrid approach is proved. Let's note that this hybrid method, intent of this paper, requires less numerical complexity and needs less storage than the MoM method, which makes its use more practical and evidencing the effect of the geometric form. In addition by using a single test function, the size of matrix becomes 1x1 instead of 30 x 30 in case of sinusoidal test functions. The fig 11 and 12 shown the distribution current on the fss structure on X-axis fig 11 and on Y-axis fig 12, for the moment method and hybrid method. In Y-axis, the draw of hybrid method overlap it's of the moment method.

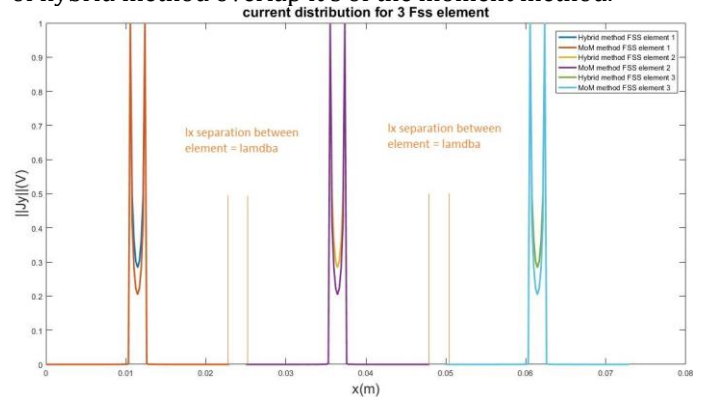


Figure 12. Current Distribution on the three FSS Element on X-axis

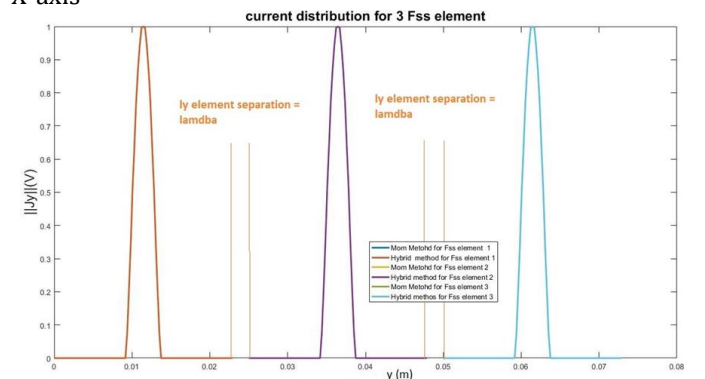


Figure 13. Current Distribution on the three FSS Element on Y-axis

In the following, we present the gain that our new approach, gives in terms of convergence and time calculation against the reference (MoM) method. Table 1 and Table 2 summarizing the benefits of our approach. Table 1 represents the number of tests and modal basis functions needed to obtain the convergence of input impedance for the range [8GHz, 12GHz], (shown in figure 6) and gives also the required time needed, for two values of Diffraction

Coefficient D1 and D2 for different angle of observation $\varphi_1 = \pi$ respectively, $\varphi_2 = \pi$. In fact to calculate the input impedance we need 16.78 s using our hybrid method, respectively 1431.569 s using MoM Method with sinusoidal test function. Further, by using our approach for the analysed structure, only 100 waveguide's modes are required to obtain the convergence. Respectively, 3000

waveguides modes and 16 test function for MoM Method to obtain the convergence. Hence, Table 2 gives the time in seconds of calculation and the number of test and basis function needed to get the convergence of the study structure when evaluating the current and electric fields. We accomplish the comparison between the MoM and the hybrid approach.

Table1. Comparison of computing time consumed between the MoM and hybrid approach to computing Zin input impedance in the range [8-12GHz] for A unit Fss Element (P: Number of test functions and N = Number of Basis functions)

Used Method	Time for D1	Time D2	Conv. for D1	Conv. for D2	All Element
MoM Method	320	322	P=16 N=3000	P=16 N=3000	$(Q * M) * (P + N)$
Hybrid Method	15.65	15.75	P=1 N= 100	P=1 N= 100	$(Q * M) * (P + N)$

Table2. Comparison of time consumed between the MoM and hybrid approach to computing the current distribution for A unit Fss Element (P: Number of test functions and N = Number of Basis functions)

Used Method	Time for D1	Time D2	Conv. for D1	Conv. for D2	All Element
MoM Method	1320	1322	P=16 N=3000	P=16 N=3000	$(Q * M) * (P + N)$
Hybrid Method	25.65	25.51	P=1 N= 100	P=1 N= 100	$(Q * M) * (P + N)$

As we concluded from this 2 tables, for an Fss Structure of $(N * Q)$, time is multiplied by the fss's dimension. The hybrid approach indulges a considerable reduction and enhancement of the operation time, in addition, the number of modes to obtain convergence is considered reduced, these important advantages are guaranteed by the use of a single test function. Proportionally, when the number of test function decreases, the size of the manipulated matrices decreases. The computational time will be reduced exponentially.

4. Conclusion

In this paper, we present a new Hybrid method that we lead a much less operation, and to reach the convergence quickly and faster than MoM Method because we use a single test function. This hybrid method is applied to Fss's structure with $(Q * M)$ dimension. Therefore, in free space, and for certain frequency range, tying Diffraction phenomena of these EM waves and its interaction with the complex form of this structures explored more the properties of FSS and correct some parameters.

We demonstrate in this paper:

- The link among their crucial theoretical, structure geometry and significant performance parameters due to Diffraction phenomena analyze;
- A joining numerical method with asymptotic one General Theory Of Diffraction (GTD) in the new approach of analyzing;
- Highlight the important of Diffraction phenomena on their performance.

A new hybrid method combines the two asymptotic method the (PO) Optical physic and (GTD) General theory of Diffraction, the first applies to the surface of the antenna and gives us the distribution of the current, in this area to this

function which models the shape of the current we add that determined by the GTD the second one, so we have an accuracy and complete function then we introduce the effect of the shapes by using the diffraction coefficient. Consequently, the size of the operation manipulated in the matrices is enormously reduced. As the result of this, we reduce the numerical complexity and memory, CPU resources required for the problem.

References

- [1] Tretyakov, S.A.; Glybovski, S.B.; Belov, P.A.; Kivshar, Y.S.; Simovski, C.R. Meta- surfaces: From microwaves to visible. Phys. Rep. 2016, 634, 1–72.
- [2] Munk, B.A. Frequency Selective Surfaces: Theory and Design; Wiley Online Library: Hoboken, NJ, USA, 2000; Volume 29.
- [3] Costa, F.; Monorchio, A.; Manara, G. An overview of equivalent circuit modeling techniques of frequency selective surfaces and metasurfaces. Appl. Comput. Electro- magn. Soc. J. 2014, 29, 960–976.
- [4] Gianvittorio, J.P.; Romeu, J.; Blanch, S.; Rahmat-Samii, Y. Self-similar prefractional frequency selective surfaces for multiband and dual-polarized applications. IEEE Trans. Antennas Propag. 2003, 51, 3088–3096.
- [5] Kern, D.J.; Werner, D.H.; Monorchio, A.; Lanuzza, L.; Wilhelm, M.J. The design synthesis of multiband artificial magnetic conductors using high impedance frequency selective surfaces. IEEE Trans. Antennas Propag. 2005, 53, 8–17.
- [6] Yang, F.; Rahmat-Samii, Y. Electromagnetic Band Gap Structures in Antenna Engineering; Cambridge University Press: Cambridge, UK, 2009.
- [7] Kunz, K.S.; Luebbers, R.J. The Finite Difference Time Domain Method for Elec- tromagnetics; CRC Press: Boca Raton, FL, USA, 1993.
- [8] Bagby, J.S.; Nyquist, D.P.; Drachman, B.C. Integral formulation for analysis of integrated dielectric waveguides. IEEE Trans. MTT-33 1985, 33, 906–915.
- [9] Koshiba, M.; Suzuki, M. Application of the Boundary-Element Method to Wave- uide Discontinuities (Short Paper). IEEE Trans. Microw. Theory Tech. 1986, 34, 301–307.

- [10] Mink, J.W.; Schwering, F.K. Special Issue on Numerical Methods. IEEE Trans. Microw. Theory Tech. 1985, MTT-33, 10.
- [11] Chen, C.-C. Transmission through a conducting screen perforated periodically with apertures. IEEE Trans. Microw. Theory Tech. 1970, 18, 627–632.
- [12] Mittra, R.; Chan, C.H.; Cwik, T. Techniques for analyzing frequency selective surfaces—a review. Proc. IEEE 1988, 76, 1593–1615.
- [13] Orta, R.; Tascone, R.; Zich, R. A unified formulation for the analysis of general frequency selective surfaces. Electromagnetics 1985, 5, 307–329.
- [14] Bozzi, M.; Perregrini, L. Efficient analysis of thin conductive screens perforated periodically with arbitrarily shaped apertures. Electron. Lett. 1999, 35, 1085–1087.
- [15] Costa, F.; Monorchio, A.; Manara, G. Efficient analysis of frequency-selective surfaces by a simple equivalent-circuit model. IEEE Antennas Propag. Mag. 2012, 54, 35–48.
- [16] Panwar, R.; Lee, J.R. Progress in frequency selective surface-based smart electromagnetic structures: A critical review. Aerosp. Sci. Technol. 2017, 66, 216–234. [CrossRef]
- [17] Wang, J.; Qu, S.; Li, L.; Wang, J.; Feng, M.; Ma, H.; Du, H.; Xu, Z. All-dielectric metamaterial frequency selective surface. J. Adv. Dielectr. 2017, 7, 1730002. [CrossRef]
- [18] Mackay, A.; Sanz-Izquierdo, B.; Parker, E.A. Evolution of frequency selective surfaces. FERMAT 2014, 2, 1–7.
- [19] Thakur, S.; Yadava, R.; Das, S. A review on Adaptive Frequency Selective Surfaces (AFSS) based patch antennas. In Proceedings of the Computing, Communications and IT Applications Conference (ComComAp), Hong Kong, China, 1–4 April 2013; pp. 120–124.